International Journal of GEOMATE, Dec, 2022, Vol.23, Issue 100, pp.118-125
ISSN: 2186-2982 (P), 2186-2990 (O), Japan, DOI: https://doi.org/10.21660/2022.100.g12211
Geotechnique, Construction Materials and Environment

EVALUATION OF THE FAILURE INITIATION AND MODES OF FAILURE OF THE HOEK-BROWN ROCK MASS SURROUNDING UNDERGROUND STORAGE WITH HIGH INTERNAL PRESSURE

Apiwish Thongraksa[1], *Pornkasem Jongpradist[2]

[1]Department of Civil Engineering, Faculty of Engineering, Rajamangala University of Technology Krungthep, Bangkok 10120, Thailand

[2]Construction Innovations and Future Infrastructures Research Center, Department of Civil Engineering, Faculty of Engineering, King Mongkut's University of Technology Thonburi, Bangkok 10140, Thailand

*Corresponding Author, Received: 12 April 2022, Revised: 09 Dec. 2022, Accepted: 15 Dec. 2022

ABSTRACT: The critical issue for the design of highly pressurized caverns is the uplift failure. A reasonable evaluation of the failure path including the initial failure location and direction of the crack propagation is needed. A series of numerical analyses based on the finite element method was conducted in the framework of the 2D axisymmetric model by considering the variety of rock mass properties, cavern depth, and in-situ stress ratio. The wide range of the natural rock mass properties (rock strength) and initial stress conditions surrounding the cavern, which include in-situ stress ratio and depth of tunnel were considered in this investigation. To detect the location of failure initiation and distinguish the failure modes between tensile and shear failure, the tensile failure and Hoek-Brown failure criteria are utilized, respectively. The numerical results indicated that the rock strength has a strong effect on the initial failure mode while the initial failure location strongly depends on the in-situ stress ratio and rock strength. The charts of failure mode and initial failure location were created by using the relationship between unconfined compressive strength and tensile strength of rock mass and initial stress condition, respectively

Keywords: Failure mode, Uplift failure pattern, Rock failure, High pressurized cavern

1. INTRODUCTION

The large renewable energy storage with lined rock caverns (LRC) is becoming the popular alternative solution to provide stable energy sources of base load electricity [1]. When the power demand period is low, the high-pressure nature of air or gas is absorbed by the driving compressor with excess electric energy. The high-pressure air or gas is stored underground. During the peak period, high-pressure air or gas can be released into the generator to generate electrical energy for supplying the increase in the power demand. With the high internal pressure storage and relatively small underground cavern depth, the stability of rock mass above the underground cavern caused by the uplift can be a critical issue that needs to be considered [2].

For preliminary evaluation, the limit equilibrium models have been proposed to evaluate the ground uplift failure of high-pressurized gas or air caverns [3,4]. The models include the rigid cone model [5], the log spiral model [6], and the straight failure plane geometry model [4]. In these models, they do not consider the initial stress state of the surrounding ground before excavation and operation, which can lead to unrealistic evaluation. In the last decade, many researchers have performed analyses to suggest a reasonable uplift failure pattern [7–12]. According to their study, the initial failure point along the cavern periphery depends on the in-situ stress ratio that can lead to different uplift failure patterns [2,9]. The linear failure criterion model, Mohr-Coulomb, is mainly used in numerical analysis due to its simple form. To investigate the rock behavior with a wide range of stress, the linear Mohr-Coulomb may present unrealistic behavior, which can affect the factor of safety obtained from the analysis.

Many failure criteria have thus been proposed to assess rock strengths more reasonably. Among several criteria, the nonlinear failure model based on the Hoek-Brown (H-B) criterion [13] is one of the most popular models. In recent years, the H-B criterion has been proven to be able to better describe the nonlinear rock mass behavior and is widely utilized in engineering practices [14], road cuts and cliff face stability analysis [15]. However, the H-B failure criterion was developed to capture only the shear failure mode. Generally, the rock mass can fail both tensile and shear failures [16], which may lead to different uplift failure path evaluations.

In this article, the failure behavior of rock mass around a pressurized cavern is investigated by considering the initial failure mode and location. A series of numerical analyses are conducted by taking

to account the variety of rock mass properties, cavern depth, and in-situ stress ratio. The H-B criterion and tensile criterion are used to determine rock failure. A conceptual guideline for predicting the failure mode of rock mass and the possible location of a failure initiation along the cavern periphery with considering the rock strength and initial stress state is established in this study

2. RESEARCH SIGNIFICANCE

To get a better understanding of the uplift failure of the surrounding rock mass containing a high-pressure storage cavern for a wide range of stress, the nonlinear failure criterion is required. Three influencing factors including depth of cavern, in-situ stress ratio, and rock mass strength are taken into account in this investigation to identify the initial failure mode and location of the initial failure, which may lead to different uplift failure patterns. This investigation provides the guideline information for predicting the initial mode of failure and location of failure initiation along the cavern periphery in engineering practical design and analysis.

3. FAILURE MECHANISM

The rock material can be failed under the tension or shear failure modes. For tensile failure, when the value of tensile stress reaches the critical value of the material, failure occurs. The simple equation can be written as

$$\sigma_1 - \sigma_T = 0 \quad (1)$$

When σ_1 and σ_3 are the major and minor principal stress, and σ_T is the tensile strength of the material (tension is positive).

For the shear failure criterion, the Hoek and Brown (H-B) model was adopted. The general form of H-B failure criterion can be mathematically expressed in terms of the major and minor principal stress as

$$\sigma_{3HB} = \sigma_1 + \left(-m_i \sigma_c \sigma_1 + s\sigma_c^2\right)^{0.5} \quad (2)$$

The m_i and s are the constant values that depend on the properties of the rock mass. The unconfined compressive strength (UCS) of rock represents by the σ_c in the equation. For intact rock material, s = 1.0. The shear failure occurs when the stress state which is represented by the Mohr circle reaches the shear failure envelope determined by the H-B model as displayed in Fig. 1. The minor principal stress calculated from the H-B model in Eq. 2 (σ_{3HB}) can be determined using the stress state and rock strength. According to Fig.1, the shear failure occurred under the condition of σ_{3HB}/σ_3 equal to 1. The failure ratio used in this investigation can be expressed as

$$\frac{\sigma_{3HB}}{\sigma_3} = \frac{\sigma_1 + \left(-m_i \sigma_c \sigma_1 + \sigma_c^2\right)^{0.5}}{\sigma_3} = 1.0 \quad (3)$$

4. NUMERICAL ANALYSIS

4.1 Problem Characteristic

In this investigation, the 2D axisymmetric problem is considered. The analytical model and loading condition are demonstrated in Fig. 2. The silo cavern has a diameter of 22.2 m. and 33.3 m in high. The depth of cavern storage is located at a depth in the range of 60 – 150 m. The bottom boundary was constrained in both lateral and vertical directions. Boundaries on both vertical sides were fixed in only one direction, which does not allow them to move in the lateral direction. The properties of rock mass used in the numerical model can be divided into 2 groups including the control properties and varying properties. The unit weight of rock (γ), Young's modulus (E), and Poisson's ratio (ν) are fixed as shown in Table 1. Regarding the literature review, [17] collected the properties of rock mass of 28 different types of rock from many researchers. The range of the unconfined compressive strength and m value of rock exhibited in the range of 37.2 – 264.8 MPa and 3.2 – 54.6. Therefore, in the sensitivity analyses, the ranges of unconfined compressive strength of rock and the m value are considered between 1 to 300 MPa and 5 – 25, respectively. Moreover, the influencing factor that strongly affects the initial failure location as discussed in the work of [2], the in-situ stress ratio (k) is also taken into account in the range of 0.3 – 3.0.

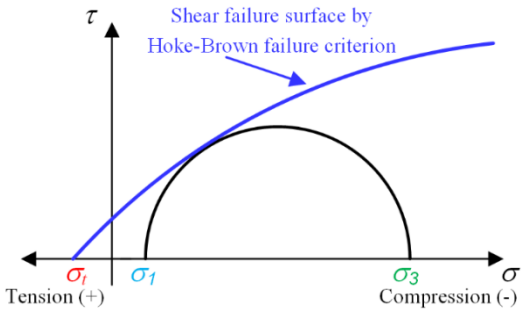

Fig. 1 Shear failure proposed by Hoek-Brown

4.2 Procedures for Detection of Initial Failure

A series of stress analyses by using the continuum finite element program ABAQUS (2016) of the cavern under increasing internal pressure is performed to determine the failure initiation location. The analysis procedures can be divided into 3 steps from the initial to operation stages which are the in-situ stress state generation, the silo cavern excavation, and applied internal pressure to simulate the

Table 1 Controlled rock properties

Quantity	Symbol	Value	Unit
Unit weight	γ	26	kN/m^3
Young modulus	E	6.66	GPa
Poisson's ratio	ν	0.2	-

underground cavern storage state. The level of internal pressure increases until the deviator stress along the cavern storage achieves the shear failure criterion, the value of the maximum major principal stress and the location of maximum σ_1 and minimum of σ_{3HB}/σ_3 are captured.

4.3 The Notion of the Failure Mode Identification

The stress state in the rock mass surrounding the silo chamber gradually changes both principal and deviatoric stresses as the internal pressure increases. The stress along the cavern wall, radial stress, becomes compression while the stress in the perpendicular direction, tangential stress, becomes tension as represented as σ_3 and σ_1 , respectively. Therefore, the radius of the Mohr circle increases with the increase of internal pressure. When the Mohr circle reaches the failure envelope surface which is determined by the H-B model of σ_{3HB}/σ_3 = 1.0, the shear failure occurred. If the tensile strength of rock mass is equal to the maximum major principal stress at σ_{3HB}/σ_3 = 1.0, the failure initiation occurs under shear and tension simultaneously. For rocks that have greater tensile strength, the shear failure mode can be obtained while the rock with a lower tensile strength than the value of σ_1 at σ_{3HB}/σ_3 = 1.0, the failure initiation caused by tensile mode is induced.

5. NUMERICAL RESULTS

5.1 Influence of the Rock Properties on Initial Failure Mode for Underground Cavern Storage

The effects of the rock strength and types of rock mass on the induced failure are described in this section. Fig. 3 presents the major principal stress distribution at the occurrence of shear failure under the operation state. It can be noticed that the minimum of σ_{3HB}/σ_3 and the maximum major principal stress exhibited at the same location for the example case (cavern depth of 60 m. and k of 1). With the rock having greater ultimate compressive strength, the required level of pressure inside the cavern storage (P_{cav}) is increased. The location of the initial failure tends to move from cavern crown to cavern sidewall while the location of maximum σ_1 and minimum σ_{3HB}/σ_3 are still the same locations. If the ultimate tensile strength of rock is equal to maximum σ_1, the initial failure is induced under shear and tensile modes simultaneously.

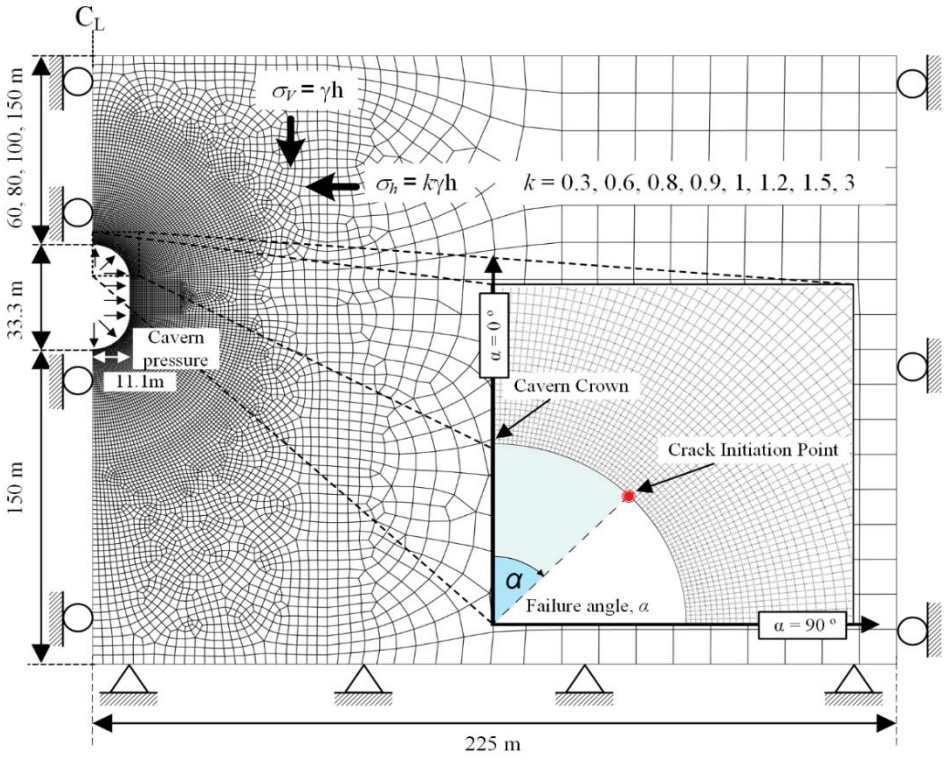

Fig.2 The loading and boundary conditions of the analytical model.

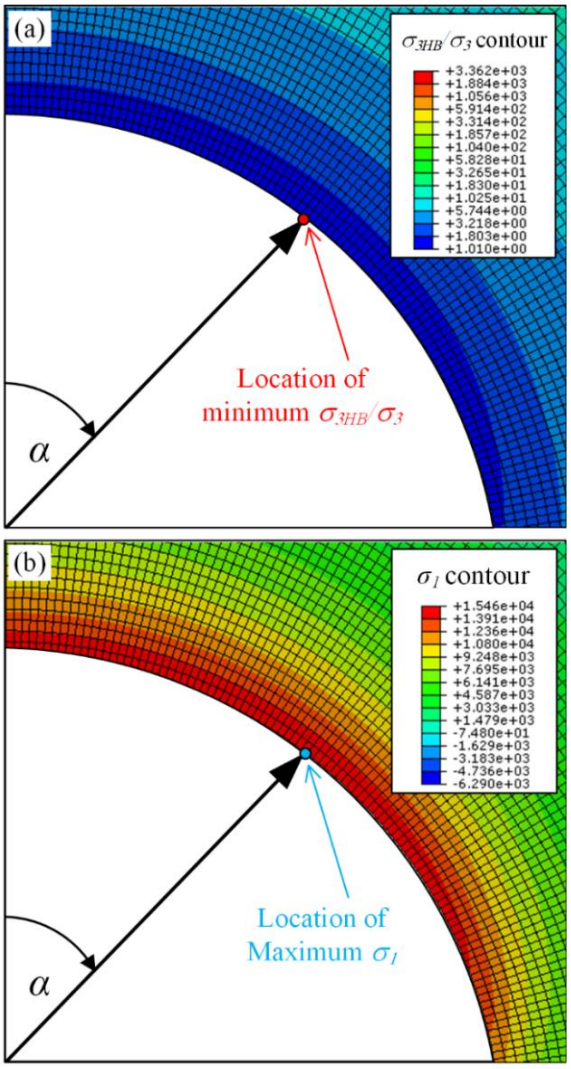

Fig. 3 The location of (a) the minimum value of $\boldsymbol{\sigma_{3HB}/\sigma_3}$ and (b) the maximum $\boldsymbol{\sigma_1}$ with internal pressure of 32.6 MPa.

From the simulation results in the case of cavern depth of 60 m. and k = 1, the data points which are the relationship between ultimate compressive strength and tensile strength under shear and tensile failure occurs simultaneously, are plotted as shown in Fig. 4. The further investigations were conducted to get a better understanding of the effect of rock strength by considering rock compressive strength in the range of 1 to 300 MPa and m_i-value of 5, 10, and 25. By collecting all the relationships between the rock unconfined compressive strength and the major principal stress (tensile strength) at the occurrence of shear failure in all analysis cases, the boundary line to distinguish the mode of failure can be obtained as shown in Fig. 5. According to the results, it can be seen that the rock mass strength has a strong effect on the initial failure mode. The rock with the properties (shear and tensile strengths) locates above the boundary line, the tensile failure is dominated at the initial failure. While the initial failure mode is governed by shear if the rock strength properties locate under the boundary line. To increase the reliability of the analysis results, the rock mass properties used in the physical model test in Thongraksa et al. [9] are plotted in the figure by considering the scaling factor. In their work, the triaxial tests were performed to determine the synthetic rock properties used in the experiment. By using the Hoek-Brown failure criterion to determine the shear failure envelope, the m_i-value and UCS can be calculated, which are equal to 17.78 and 43.95 kPa. It can be seen that the expected initial failure mode is the shear failure, which shows a good agreement with the previous study. Therefore, the chart of initial failure mode with nonlinear criterion has been proven to predict the failure of rock mass in underground cavern storage with high pressure.

5.2 The Initial Failure Location Assessment of Underground High-Pressure Storage

Three factors, the depth of the cavern, in-situ stress ratio, and rock strength are taken into account in the analysis to determine the initial failure location. Fig. 6 shows the initial failure locations in the cases of cavern depth of 60 m and k of 0.3, 1, and 3, which represent the in-situ stress ratio of less than, equal to and more than 1 by varying the *UCS* in the range of 50 to 250 MPa. In the case of k of less than 1, the initial failures occur at the cavern roof while for the k larger than 1, the initial failures are located at the cavern sidewall. In case of k become unity, the initial failure location can be captured between the cavern roof and sidewall which has a failure angle in the range of 30° and 40°. In addition, the required pressure level also increases with the rock having greater strength. It is seen that the initial failure location depends on the rock mass strength. Similar results were also obtained in previous studies [9,18]. To get a better understanding of the initial failure location of the rock, the in-situ stress in a range of 0.3 to 3.0 and the depth of the cavern in the range of 60 to 150 m are chosen to perform the further investigation. The analyzed initial failure location are plotted in a radial space concerning the rock mass strength (tensile and shear strengths), as illustrated in Fig. 7. To eliminate the influence of cavern depth, both terms of shear and tensile strengths are normalized by the vertical stress. As seen in Fig. 7, the rock strengths have a strong effect on the initial failure location for cases with k in the range of 0.8 – 1 for the low rock strength. Moreover, for cases of k less than 0.8, the initial failure locations are located at the cavern roof while in cases of k larger than 1, the locations of initial failure occur at the cavern side wall.

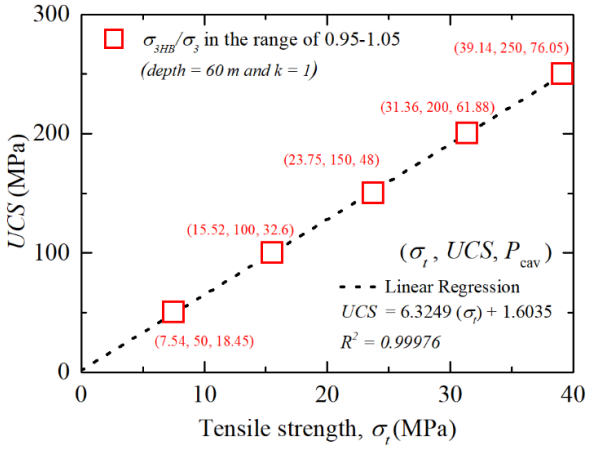

Fig. 4 The relationship between shear strength and tensile strength at both shear and tension failures occur simultaneously.

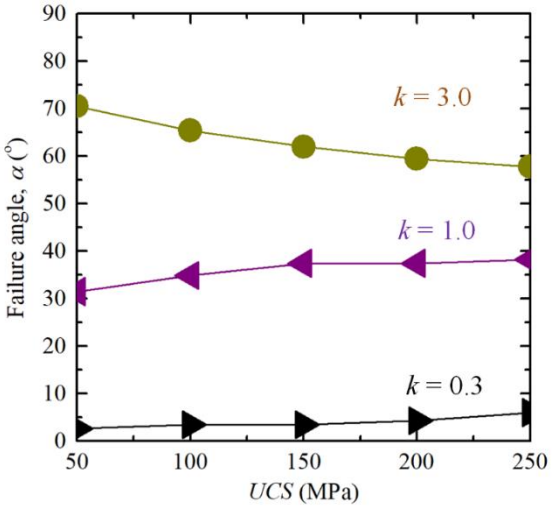

Fig. 6 The relationship between unconfined compressive strength (*UCS*) and failure angle (α) at depth of craven of 60 m.

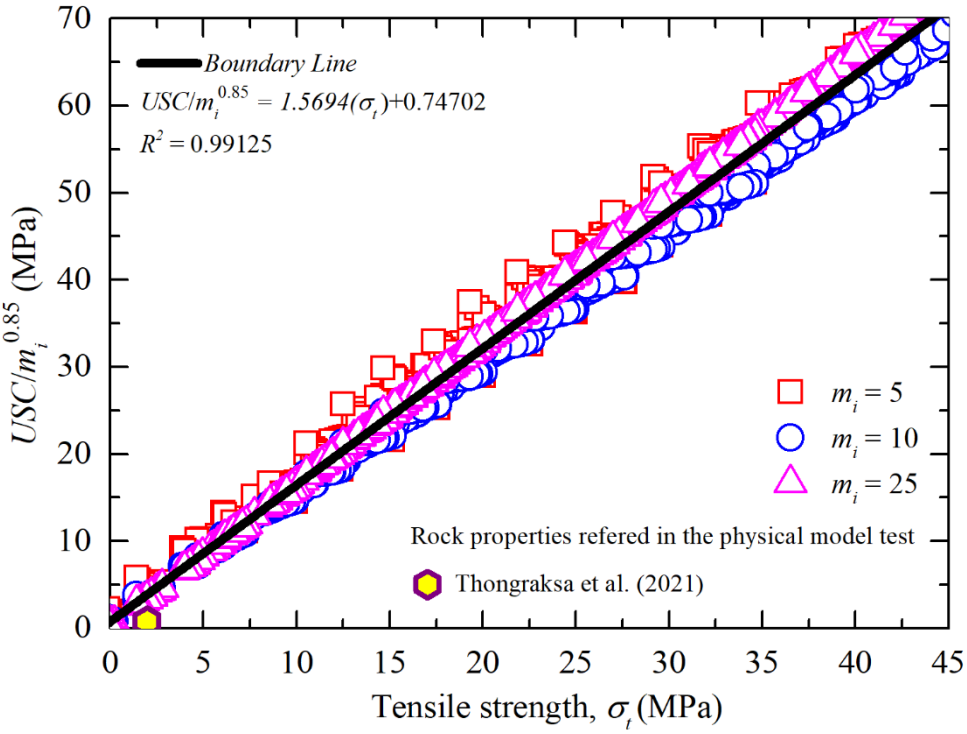

Fig. 5 The chart for classifying the initial failure mode.

With increasing rock strength, the location of the initial failure tends to approach the cavern shoulder which has a failure angle of approximately 40°. After investigating all influencing factors, the practically simple chart for determining the initial failure location is proposed as demonstrated in Fig 8. By knowing the mode of failure from the chart of the mode of failure as presented in Fig 5, to find the expected failure location, one can start with the horizontal or vertical axis for the tensile failure and shear failure, respectively. Subsequently, by projecting in the circumferential direction to the line which represents the in-situ stress ratio, the initial failure angle can be obtained by reading the failure angle from the corresponding radial axis.

To validate the proposed chart, the scale-down model tests for the case of underground storage with internal pressure conducted by Thongraksa et

al. [9] are chosen. In their work, the initial failure occurred under shear failure both *k* of 1 and 3 with a depth of 40 m for the full-scale problem. The initial failure angle for *k* of 1 and 3 are 45° and 75°, respectively. In Fig. 8, the failure initiation points for both cases are added to the chart by plotting the relationships between the terms of shear strength and initial failure angle. In the case of *k* larger than 1, a good agreement between the physical model test and the proposed chart can be obtained. The small discrepancy between the failure angle captured in the experiment and the prediction chart is exhibited in the case of *k* equal to 1 because the failure angle is very sensitive to low rock strength under this *k*. It can be concluded that the proposed chart for determining the failure location shows reasonable agreement with the experimental results.

6. CONCLUSION

This investigation presents the initial failure behavior of rock mass surrounding the underground cavern storage with high internal pressure via a series of numerical analyses. The effect of the cavern depth, in-situ stress ratio, and rock mass strengths on the initial failure and mode of failure by using nonlinear failure criterion, Hoke-Brown failure are conducted. The main finding of this investigation can be summarized as follows;

1. The initial failure mode strongly depends on rock mass strengths which are the relationship

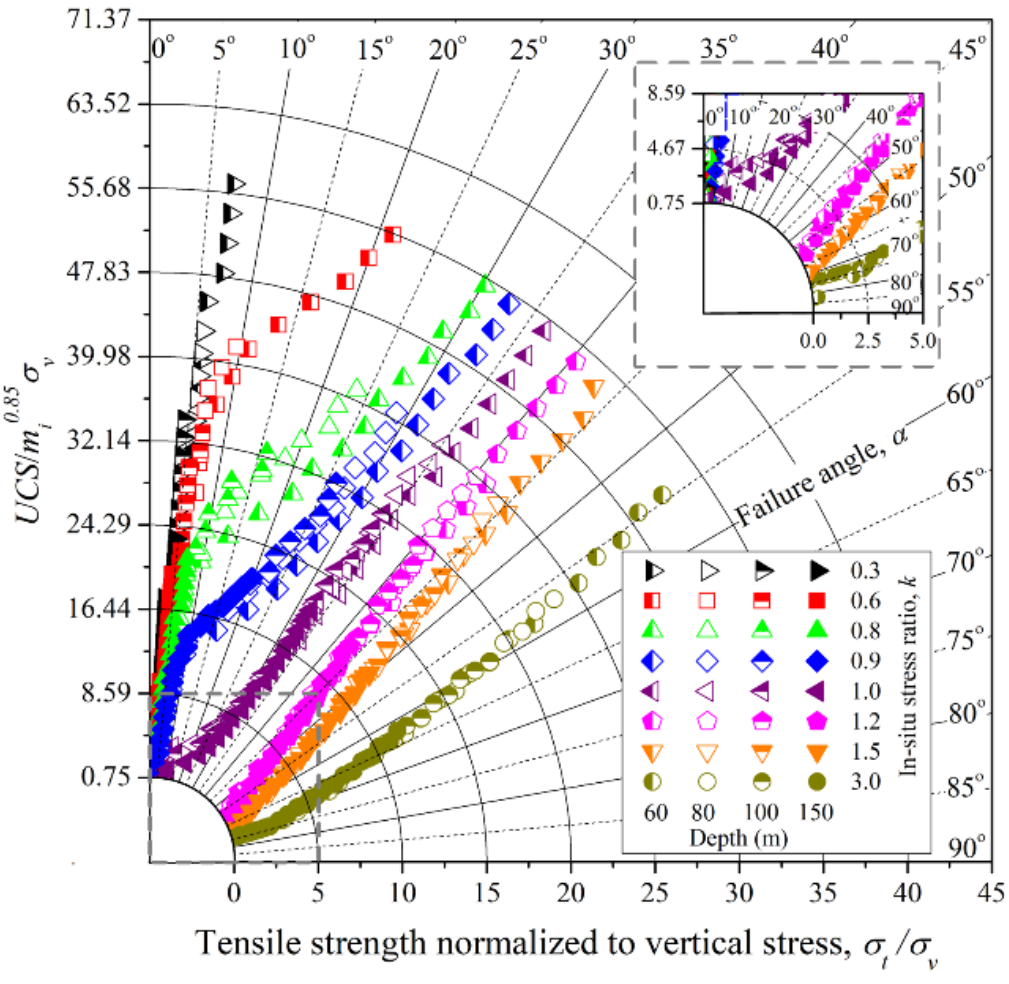

Fig. 7 Effect of the rock strength and stress state on the initial failure location.

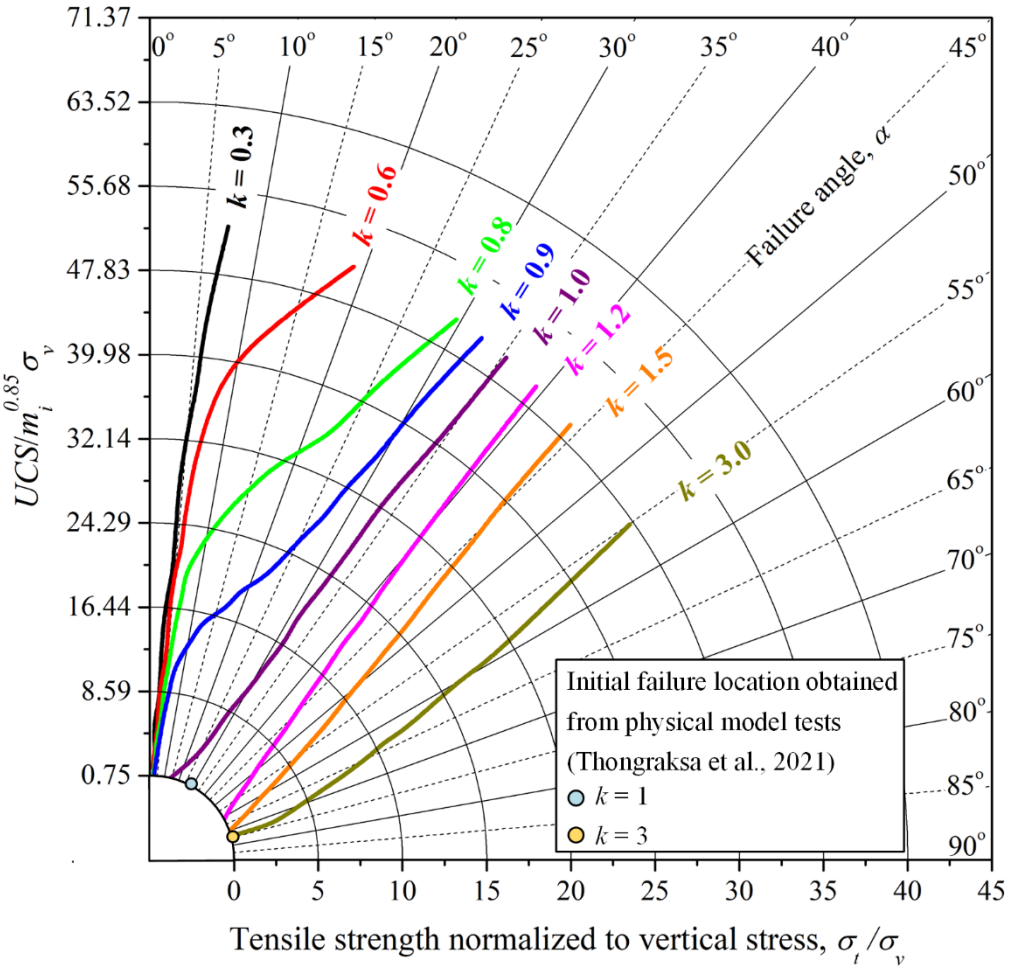

Fig. 8 Chart for predicting the location of initial failure, accounting for the rock mass strength, cavern depth, and in-situ stress ratio.

between shear strength and tensile strength. By considering the range of the natural rock properties, the boundary line to separate the tensile and shear failure modes can be obtained. The initial failure mode can be expected by knowing the rock mass strengths.

2. The initial failure location is governed by three influencing factors consisting of rock strength, depth of cavern, and initial in-situ stress ratio. Among these, the depth of the cavern has the smallest effect on the initial failure point. In low rock strength, the in-situ stress ratio has a strong effect on the initial failure location. For high rock strength, the initial failure location seems to locate in the zone between the cavern roof and sidewall.

3. The charts for expecting the failure mode from the rock strengths and for determining the failure location from its influencing factors are proposed and preliminarily verified. The charts can be practically useful in the early stage of high-pressurized cavern design.

7. ACKNOWLEDGMENT

This research work was supported by Thailand Science Research and Innovation (TSRI) under Fundamental Fund 2023 (Project: Advanced Construction Towards Thailand 4.0).

8. REFERENCES

[1] Salgi G., Lund H., System behaviour of compressed-air energy-storage in Denmark with a high penetration of renewable energy sources, Appl. Energy, Vol. 85, No. 4, 2008, pp. 182–189.

[2] Tunsakul J., Jongpradist P., Kongkitkul W., Wonglert A., Youwai S., Investigation of failure behavior of continuous rock mass around cavern under high internal pressure, Tunn. Undergr. Sp. Technol., Vol. 34, 2013, pp. 110–123.

[3] Brandshaug T., Christianson M., Damjanac B., Technical review of the lined rock cavern (LRC)

concept and design methodology—mechanical response of rock mass, Technical Report ICG01-2062-1-4. Itasca Consulting Group, Inc, 2001.
[4] Japan Gas Association, Development of advanced natural gas storage technology. Ann. Rep., 2008, pp. 3–9.
[5] Littlejohn G.S., Bruce D.A., Rock anchors—state of the art. Part 1: Design (1). Ground Eng., Vol. 8, 1975, pp. 25–32.
[6] Ghaly A., Hanna A., Ultimate pullout resistance of single vertical anchors. Can. Geotech J., Vol. 31, 1994, pp. 661–672.
[7] Tunsakul J., Jongpradist P.,Soparat P., Kongkitkul W., Nanakorn S., Analysis of fracture propagation in a rock mass surrounding a tunnel under high internal pressure by the element-free Galerkin method, Comput. Geotech., Vol. 55, 2014, pp. 78–90.
[8] Kim H.M., Park D., Ryu D.W., Song W.K., Parametric sensitivity analysis of ground uplift above pressurized underground rock caverns, Eng. Geol., Vol. 135-136, 2012, pp. 60–5.
[9] Thongraksa A., Punya-in Y., Jongpradist P, Kim H.M., Jamsawang P. Failure behaviors of rock masses around highly pressurized cavern: Initiation and modes of failure. Tunn. Undergr. Sp. Technol., Vol. 115, 2021, p. 104058.
[10] Tunsakul J., Jongpradist P., Kim H.M., Nanakorn P., Evaluation of rock fracture patterns based on the element-free Galerkin method for stability assessment of a highly pressurized gas storage cavern, Acta. Geotech., Vol. 13, 2018, pp. 817–832.
[11] Wang H.T., Liu P., Li S.C., Li X.J., Zhang X., Limit analysis of uplift failure mechanisms for a high-pressure gas storage tunnel in layered Hoek-Brown rock masses, Eng. Fail. Anal., Vol. 138, 2022, p. 106274.
[12] Jongpradist P., Tunsakul J., Kongkitkul W., Fadsiri N., Arangelovski G., Youwai S., High internal pressure induced fracture patterns in rock masses surrounding caverns: Experimental study using physical model tests, Eng. Geol., Vol. 197, 2015, pp. 158–171.
[13] Hoek E., Brown E., Underground excavations in rock The Institution of Mining and Metallurgy, 1980.
[14] Zhao J., Applicability of Mohr-Coulomb and Hoek-Brown strength criteria to the dynamic strength of brittle rock, Int J. Rock Mech. Min. Sci., Vol. 37, 2000, pp. 1115–21.
[15] Lindsay P., Campbell R.N., Fergusson D.A., Gillard G.R., Moore T.A., Slope stability probability classification, Waikato Coal Measures, New Zealand. Int. J. Coal. Geol., Vol. 45, 2001, pp. 127–45.
[16] Paterson M.S., Wong T., Experimental rock deformation — the brittle field, Springer, 2005.
[17] He M., Zhang Z., Zheng J., Chen F., Li N., A New Perspective on the Constant mi of the Hoek–Brown Failure Criterion and a New Model for Determining the Residual Strength of Rock, Rock Mech. Rock Eng., Vol. 53, 2020, pp. 3953–3967.
[18] Perazzelli P., Anagnostou G., Upper bound limit analysis of uplift failure in pressurized sealed rock tunnels, Int J Numer Anal. Methods Geomech., Vol. 42, 2018, pp. 719–735.